Effect of driving frequency on the structure of silicon grown on Ag (111) films by very-high-frequency magnetron sputtering*

Jia-Min Guo(郭佳敏)[1], Chao Ye(叶超)[1,2,†], Xiang-Ying Wang(王响英)[3], Pei-FangYang(杨培芳)[1], and Su Zhang(张苏)[3]

[1] College of Physics, Optoelectronics and Energy, Soochow University, Suzhou 215006, China
[2] Key Laboratory of Thin Films of Jiangsu Province, Soochow University, Suzhou 215006, China
[3] Medical College, Soochow University, Suzhou 215123, China

(Received 2 December 2016; revised manuscript received 12 February 2017; published online 20 April 2017)

The effect of driving frequency on the structure of silicon grown on Ag (111) film is investigated, which was prepared by using the very-high-frequency (VHF) (40.68 MHz and 60 MHz) magnetron sputtering. The energy and flux density of the ions impinging on the substrate are also analyzed. It is found that for the 60-MHz VHF magnetron sputtering, the surface of silicon on Ag (111) film exhibits a small cone structure, similar to that of Ag (111) film substrate, indicating a better microstructure continuity. However, for the 40.68-MHz VHF magnetron sputtering, the surface of silicon on Ag (111) film shows a hybrid structure of hollowed-cones and hollowed-particles, which is completely different from that of Ag (111) film. The change of silicon structure is closely related to the differences in the ion energy and flux density controlled by the driving frequency of sputtering.

Keywords: silicon growth, Ag film substrate, structural property, very-high-frequency sputtering

PACS: 52.80.Pi, 81.15.Cd, 68.55.J– **DOI:** 10.1088/1674-1056/26/6/065207

1. Introduction

With the development of graphene, another two-dimensional honeycomb lattice, i.e., the silicene, similar to that of graphene has attracted a great deal of attention.[1–6] However, the two-dimensional honeycomb lattice of Si cannot exist in nature as that of the graphene because the binding between silicon atoms is in the sp^3-bonded state, not in the sp^2-bonded state as that of carbon atoms. Thus, the two-dimensional honeycomb lattice of Si must be grown by epitaxial method on the metal substrate with two-dimensional honeycomb structure, such as the (111) surface of bulk crystalline Ag and the ultra-thin Ag (111) film.[3,10–14] However, the major technology currently used to grow silicene is the ultra-high-vacuum evaporation epitaxy, which requires a strict control of evaporated Si amount and substrate temperature, making the synthesis of silicene very challenging.

The pulsed or inductively coupled plasma (ICP) enhanced direct current (DC) magnetron sputtering is also an important technology for the epitaxial growth of Si film.[17–20] However, the growth of Si two-dimensional honeycomb lattice by sputtering method is seldom reported. The possible reason is the difficulty in strictly controlling the sputtered Si amount and the appropriate ion energy because the sputtered ions in the pulsed or ICP enhanced DC magnetron sputtering usually have a higher flux and lower energy. If the ion flux can be effectively reduced while the ion energy can be increased appropriately, the growth of Si two-dimensional honeycomb lattice on Ag (111) films may be achieved.

Recently, the investigations on the 60-MHz very-high-frequency (VHF) magnetron sputtering discharge have shown that the ions produced by the VHF magnetron sputtering have a very low flux density and a higher energy.[21,22] This feature is fit for the growth of Si 2D nano-structure, because the higher ions energy helps to enhance the surface diffusion of silicon adatoms, making the silicon adatoms reach a position with low surface energy,[23] while the lower ion flux can control the number of silicon adatoms onto the substrate, reducing the rapid spatial growth. This stimulates our curiosity about whether the Si 2D honeycomb lattice can be prepared by using the VHF magnetron sputtering. Therefore, in this work, the growth and structures of silicon on Ag (111) films by the 40.68-MHz and 60-MHz VHF magnetron sputterings are investigated. The results show that the two-dimensional nano-structures of silicon can be well grown on the Ag (111) films by the VHF magnetron sputtering, though the silicene cannot be obtained currently.

2. Experimental details

The experiments were carried out in an unbalanced dual-magnetron sputtering.[24] The device was a cylindrical vacuum chamber made of stainless steel (350 mm in diameter and 300 mm in height), in which a circular Ag target and a circular silicon target (both with 99.999% in purity, 50 mm in diameter, and 5 mm in thickness) were mounted on the water-cooled

*Project supported by the National Natural Science Foundation of China (Grant Nos. 11675118 and 11275136).
†Corresponding author. E-mail: cye@suda.edu.cn
© 2017 Chinese Physical Society and IOP Publishing Ltd

copper surface at the top of the chamber with the angles of 45° and 135°, respectively. The water-cooled substrate holder (100 mm in diameter) was set at the bottom, about 70 mm apart from the center of the target surface. The device was pumped down to a base pressure less than 5×10^{-4} Pa before each deposition, with a 600-l/s turbo-molecular pump backed up with a mechanical pump. Argon with a fixed flow rate of 30 sccm was used as the discharge gas and the operating pressure was maintained at 4.7 Pa–5.0 Pa. The target was pre-sputtered in Ar for 10 min prior to each run.

The preparation of samples included two steps. The first step was to deposit Ag film substrates. The Ag films were deposited on n-type (100) silicon wafers and quartz crystal wafers. The Ag target was sputtered for 30 min by using a 2-MHz radio-frequency (RF) source (not the usual 13.56-MHz RF source) at a sputtering power of 200 W, forming the Ag (111) film substrates each with a thickness of about 380 nm. The reason for preparing the Ag films by using the 2-MHz sputtering in this work was that the Ag films prepared by 2-MHz sputtering had more uniform, dense and smooth surfaces than by 13.56-MHz sputtering. The second step was to grow the silicon on Ag (111) films. After finishing each deposition of Ag films, the 2-MHz RF source was turned off. Successively, the Si target was sputtered for 30 min by using a 40.68-MHz or 60-MHz VHF source at the sputtering powers of 50 W–150 W, thus forming the samples.

The surface morphologies of the Ag film deposited on n-type (100) silicon wafer and the silicon on Ag films were measured using a Bruker Dimension Icon atomic force microscopy (AFM) in AC mode. The crystalline nature of the Ag film deposited on quartz crystal wafer was measured using the D/MAX-2000PC x-ray diffractometer with Cu K_α ($\lambda = 0.154051$ nm) radiation. The binding configurations of silicon on Ag films (deposited on n-type (100) silicon wafer) were analyzed using a Thermo Scientific ESCALAB 250 XI x-ray photoelectron spectroscope (XPS) with an energy resolution of 0.1 eV. Prior to the XPS measurement, the samples were pre-sputtered for 10 s to remove the adventitious contaminants. In order to avoid the charging effects, the XPS spectra were all calibrated using the C–C binding energy (284.8 eV) when analyzing the XPS results. The XPS peak deconvolution was attempted using a Gaussian line shape after background subtraction. In order to investigate the effect of driving frequency on silicon growth, the ion energy and ion flux density at the surface of substrate were measured using the Semion HV-2500 retarding field energy analyzer (RFEA).

3. Results and discussion

3.1. Structural properties of Ag film substrate

For the growth of silicon on Ag substrates, the crystalline nature of Ag substrate can exert an obvious influence on the growth and microstructures of silicon.[8,9] In order to grow the two-dimensional (2D) honeycomb lattice of Si or 2D silicon nanosheet, the best suitable substrate is the (111) surface of bulk crystalline Ag or the ultra-thin Ag (111) film.[3,10–14] Therefore, in this work, in order to investigate the effect of driving frequency on the growth and structure of silicon, the Ag film was also used as the substrate. Figure 1 shows the XRD spectrum of the Ag film. It can be seen that the XRD pattern includes the Ag (111), Ag (200), Ag (220), and Ag (311) diffraction peaks, thus, the Ag film has a better face-centered cubic (fcc) crystal structure. It can also be seen that the Ag (111) peak is the most intense, which implies that the preferential orientation of the Ag grains was along the crystalline direction (111).[25,26] Therefore, the Ag film used in this work has the same crystal structure as that of Ag (111) substrate used in other work.[3,10–14] Figure 2 shows the 2D and three-dimensional (3D) surface morphologies of Ag (111) film measured by AFM, each of which exhibits a small cone structure. From the AFM image, the root-mean-square (RMS) roughness of the surface for 0.5 μm×0.5 μm maps is calculated, which is 4.14 nm (for the Ag film prepared by 13.56-MHz sputtering, RMS roughness is 14.42 nm). However, no atomically flat Ag (111) film[2] is obtained here.

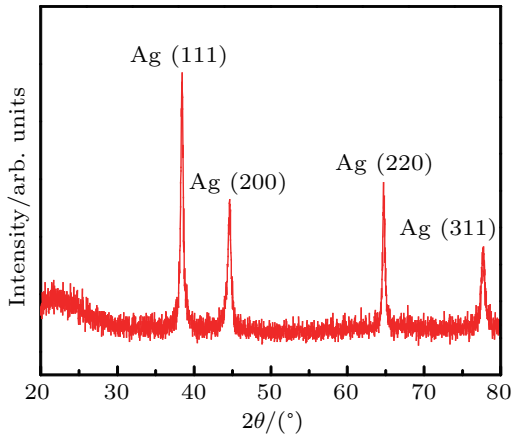


Fig. 1. (color online) XRD spectrum of Ag (111) film used as substrate.

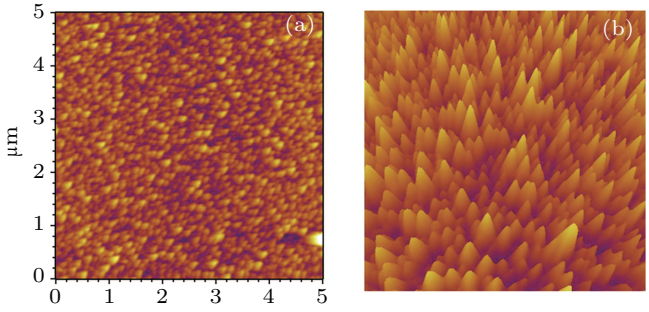


Fig. 2. (color online) AFM (a) 2D and (b) 3D height retrace images of Ag (111) film surface.

3.2. Surface morphologies of silicon on Ag (111) films

The surface morphologies of silicon on Ag (111) films are analyzed using the AFM technique. Figure 3 shows the 2D and

3D AFM height retrace images of the silicon on Ag (111) films grown using the 40.68-MHz VHF magnetron sputtering. At the sputtering power of 50 W (Figs. 3(a) and 3(b)), the sample surface consists of many hollowed-cones and many hollowed-particles (or crater-like). These hollowed-cones and hollowed-particles array along a special orientation, forming an oriented structure. This structure is completely different from that of Ag (111) film substrate. As the sputtering power increases to 150 W (Figs. 3(c) and 3(d)), the surface morphology of the sample is similar to that prepared at 50 W, but the sizes and the heights of hollowed-cones and hollowed-particles all increase. From the AFM images, the calculated RMS roughness values of samples are 2.78 nm (50 W) and 4.20 nm (150 W), respectively. These RMS roughness values are lower than or the same as those of Ag film substrates, meaning that the 2D growth of silicon along the surface of Ag film dominates the growth process.

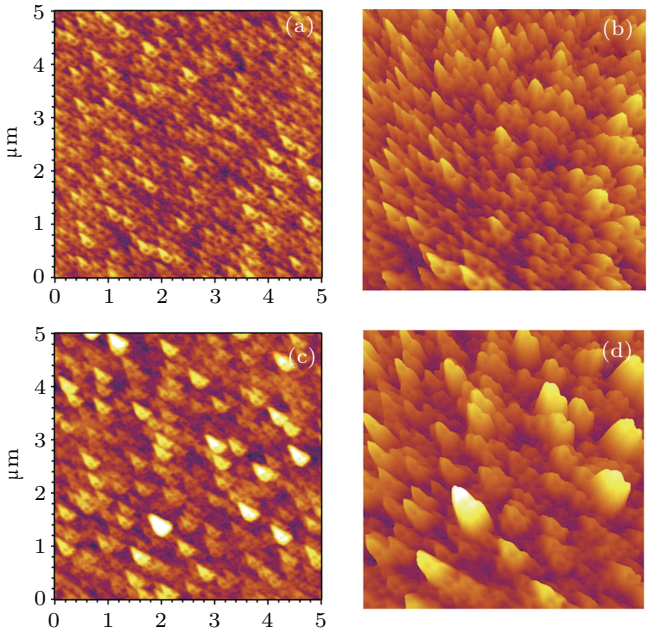


Fig. 3. (color online) AFM height retrace images of silicon on Ag (111) films sputtered by 40.68 MHz, at the powers of (a) 50 W (2D), (b) 50 W (3D) and (c) 150 W (2D), (d) 150 W (3D).

Figure 4 shows the 2D and 3D AFM height retrace images of the silicon on Ag (111) films grown using the 60-MHz VHF magnetron sputtering. At the sputtering power of 50 W, the sample surface consists of many nano-cones connected with each other along a special orientation as shown in Figs. 4(a) and 4(b). This growth feature in the special orientation is similar to that of Ag (111) film substrate, but the size of nano-cone decreases and the connectivity between the nano-cones increases. As the sputtering power increases to 150 W (Figs. 4(c) and 4(d)), the sizes of nano-cones increase and become more uniform. The surface morphology is almost the same as that of Ag (111) film substrate. From the AFM image, the calculated RMS roughness values of samples surfaces are 3.88 nm (50 W) and 4.79 nm (150 W), respectively, close to those of Ag (111) film substrates. Thus, the silicon grown on Ag (111) film substrate has a better microstructure continuity.

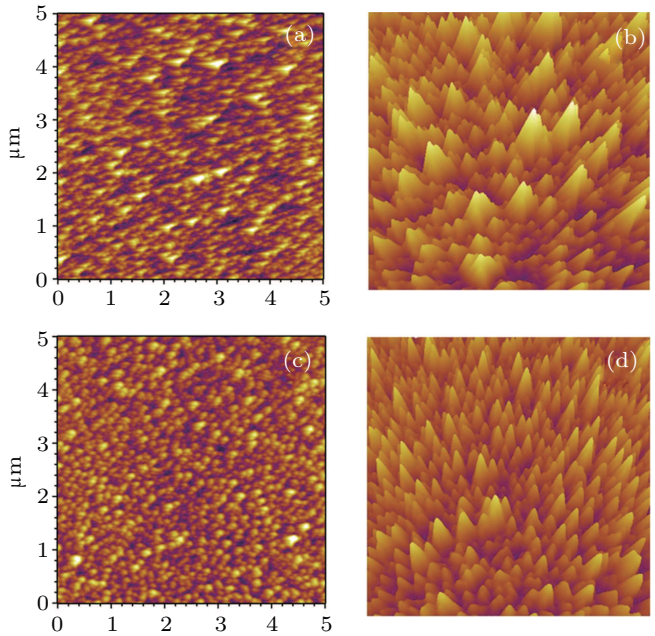


Fig. 4. (color online) AFM height retrace images of silicon on Ag (111) films sputtered by 60 MHz, at the powers of (a) 50 W (2D), (b) 50 W (3D) and (c) 150 W (2D), and (d) 150 W (3D).

3.3. XPS analysis of silicon on Ag (111) films

The binding features of samples are further analyzed using XPS. Figure 5(a) shows the Si 2p XPS peaks of the silicon on Ag (111) films sputtered by the 40.68 MHz. At the sputtering power of 50 W, the Si 2p XPS peak shows a wide single peak, then evolving into a dual-peak with the sputtering power increase. By deconvolving the Si 2p XPS peak by using a Gaussian line shape, four peaks can be fitted, which are located about 96.6 eV, 97.2 eV, 100.4 eV, and 102.7 eV, respectively. The peak at about 97.2 eV is identified as Ag 4s peak, coming from the Ag film substrate. The peak at about 100.4 eV is identified as Si–O peak coming from the reaction between sputtered silicon radicals and residual O. The other two peaks at about 96.6 eV and 102.7 eV correspond to the Si–Si sp^3-like and the sp^3 bonding peaks, respectively.[16] The Si–Si sp^3-like bonding is the incomplete sp^3 bonding in the silicon nanosheet caused by partial hybridization of the s and p_z orbitals (so-called sp^3-like hybridization).[16,27] For the silicon sputtered at 50 W, only the Si–Si sp^3-like bonding peak can be fitted, indicating the formation of silicon nanolayer because the incomplete sp^3 bonding (sp^3-like) comes from the near surface or the interface. For the silicon sputtered at 100 W–150 W, the Si–Si sp^3-like and sp^3 bonding peaks both can be fitted, and the intensity of Si–Si sp^3 bonding peak increases rapidly. This increase of Si–Si sp^3 peak intensity is related to the spatial growth of silicon, which can be proved by the increases in size and height of the hollowed-cones and hollowed-particles

as shown in Figs. 3(c) and 3(d).

Figure 5(b) shows the Si 2p XPS peaks of the silicon on Ag (111) films sputtered by the 60 MHz. It can be seen that at the sputtering power of 50 W, the Si 2p XPS peak shows a wide single peak, then with the sputtering power increase the signals at about 102 eV gradually increase. By deconvolving the Si 2p XPS peak, three peaks can be fitted, which are located about 96.4 eV, 97.4 eV, and 101.4 eV, respectively. The peak at about 97.4 eV is also from the Ag film substrate. The peak at about 101.4 eV is also the Si–O peak originating from the reaction between sputtered silicon radicals and residual O. The peaks at about 96.4 eV correspond to the Si–Si sp^3-like bonding peaks in the 2D silicon nanosheet.[16] No Si–Si sp^3 bonding peaks can be fitted. Therefore, for the silicon sputtered by 60 MHz, only the Si–Si sp^3-like bonding peak can be fitted, indicating the formation of thin silicon nanolayer because the incomplete sp^3 bonding (sp^3-like) comes from the near surface or the interface.

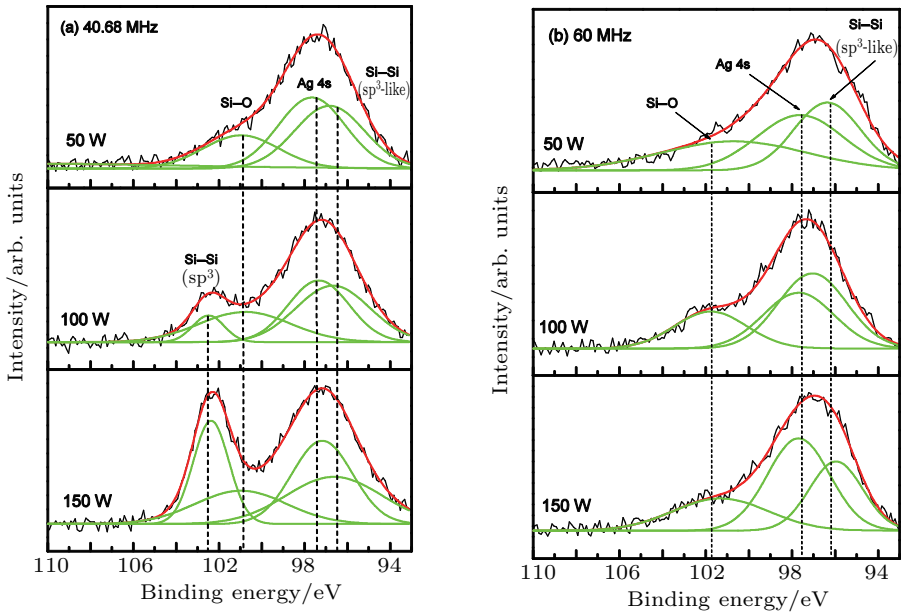


Fig. 5. (color online) Si 2p XPS peaks and their Gaussian deconvolutions of the silicon grown on Ag (111) films sputtered at (a) 40.68 MHz and (b) 60 MHz, respectively.

3.4. Ion energy and ion flux analysis of silicon growth

In order to investigate the effect of driving frequency on silicon growth, the ion energy and ion flux density on the surface of substrate are measured. Figure 6 shows the ion velocity distribution functions (IVDFs) of the 40.68-MHz and 60-MHz sputtering measured by retarding field energy analyzer. It can be found that the IVDFs all take a uni-modal shape no matter whether magnetron sputtering operates at 40.68 MHz or 60 MHz, but the ion properties (maximum ion energy and ion flux density) are different.

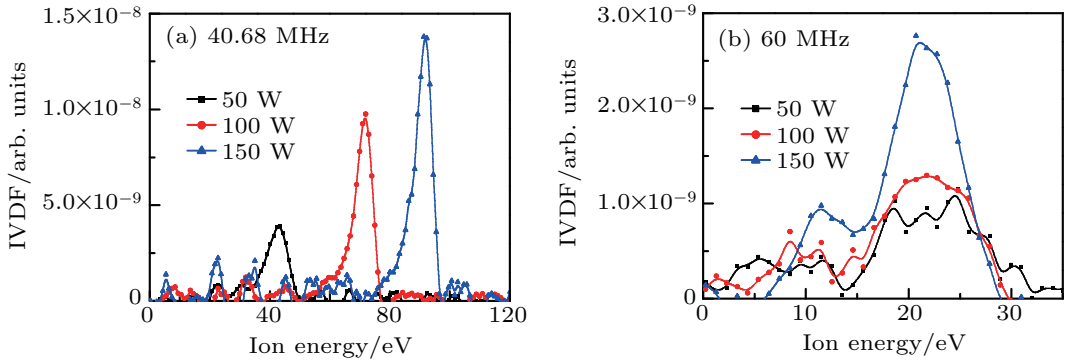


Fig. 6. (color online) IVDFs of (a) 40.68-MHz and (b) 60-MHz sputtering.

Figure 7 shows the variations of maximum ion energy and ion flux density with sputtering power. It can be found that the maximum ion energies and ion flux densities are in the ranges of 42.8 eV–91.8 eV and 0.018 A/m^2–0.057 A/m^2 for the 40.68-MHz sputtering, while in the ranges of 25.8 eV–27.9 eV and 0.008 A/m^2–0.026 A/m^2 for the 60-MHz sputtering, respectively. The maximum ion energy of 40.68-MHz sputtering is far higher than that of 60-MHz sputtering, and the ion flux density of 40.68-MHz sputtering is also higher than that of 60-MHz sputtering. For the plasma-exposed sur-

faces, the impacting of ions with higher energy can enhance the adatom surface diffusion, making the adatom reach the position with the lowest surface energy,[23] while the lower ions flux can control the amount of silicon onto the substrate, thereby reducing the rapid accumulation of adatom, thus, the 2D growth of silicon along the surface of Ag film dominates the growth process. If the ion energy is too high and the ion flux further increases, the grain growth will dominate the process. As a result, the microstructure of silicon deviates from that of the Ag (111) film substrates. Thus, the moderate ion energy and lower ion flux are needed for the 2D growth of silicon on Ag (111) film substrate.

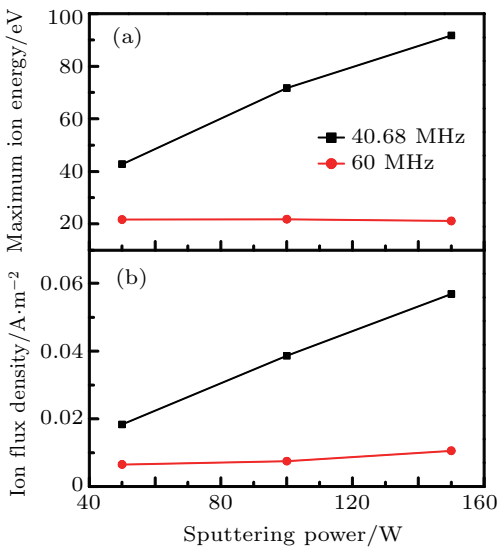


Fig. 7. (color online) Variations of maximum ion energy and ion flux density with sputtering power.

4. Conclusions

In this work, we investigated the growth and structural properties of the silicon on Ag (111) films by the 40.68-MHz and 60-MHz very-high-frequency magnetron sputterings. The energy and flux density of ions impinging the substrate are also analyzed. The results show that the growth behavior of the silicon on Ag (111) film substrate depends on the driving frequency, further on the ions energy and ions flux. For the 60-MHz VHF magnetron sputtering, the surface of silicon on Ag (111) film exhibits a small cone structure, similar to that of Ag (111) film substrate, showing a better microstructure continuity. However, for the 40.68-MHz VHF magnetron sputtering, the surface of silicon on Ag (111) film shows a hybrid structure of hollowed-cones and hollowed-particles, which is completely different from that of Ag (111) film. Therefore, a similar microstructure of silicon as Ag (111) film underlayer can be achieved by the 60-MHz VHF magnetron sputtering due to moderate ion energy and low ion flux. Although the two-dimensional honeycomb lattice of Si cannot be obtained currently, the 2D silicon nanostructures can be well grown on Ag (111) films using VHF magnetron sputtering. This encourages us to explore the possible condition to prepare the 2D Si nanolayer or silicene-like structure by using the VHF magnetron sputtering.

References

[1] Lay G L, Aufray B, Léandri C, Oughaddou H, Biberian J P, Padova P D, Dávila M E, Ealet B and Kara A 2009 *Appl. Surf. Sci.* **256** 524
[2] Sone J, Yamagami T, Aoki Y, Nakatsuji K and Hirayama H 2014 *New J. Phys.* **16** 095004
[3] Lalmi B, Oughaddou H, Enriquez H, Kara A, Vizzini S, Ealet B and Aufray B 2010 *Appl. Phys. Lett.* **97** 223109
[4] Wu K H 2015 *Chin. Phys. B* **24** 086802
[5] Wang R, Xu M S and Pi X D 2015 *Chin. Phys. B* **24** 086807
[6] Zhong H X, Quhe R G, Wang Y Y, Shi J J and Lü J 2015 *Chin. Phys. B* **24** 087308
[7] Li H, Fu H X and Meng S 2015 *Chin. Phys. B* **24** 086102
[8] Liu Z L, Wang M X, Xu J P, Ge J F, Lay G L, Vogt P, Qian D, Gao C L, Liu C and Jia J F 2014 *New J. Phys.* **16** 075006
[9] Arafune R, Lin C, Kawahara K, Tsukahara N, Minamitani E, Kim Y, Takagi N and Kawai M 2013 *Surf. Sci.* **608** 297
[10] Vogt P, Padova P D, Quaresima C, Avila J, Frantzeskakis E, Asensio M C, Resta A, Ealet B and Lay G L 2012 *Phys. Rev. Lett.* **108** 155501
[11] Fleurence A, Friedlein R, Ozaki T, Kawai H, Wang Y and Yamada-Takamura Y 2012 *Phys. Rev. Lett.* **108** 245501
[12] Feng B, Ding Z, Meng S, Yao Y, He X, Cheng P, Chen L and Wu K 2012 *Nano Lett.* **12** 3507
[13] Resta A, Leoni T, Barth C, Ranguis A, Becker C, Bruhn T, Vogt P and Lay G L 2013 *Sci. Rep.* **3** 2399
[14] Mannix A J, Kiraly B, Fisher B L, Hersam M C and Guisinger N P 2014 *ACS Nano* **8** 7538
[15] Moras P, Mentes T O, Sheverdyaeva P M, Locatelli A and Carbone C 2014 *J. Phys.: Condens. Matter* **26** 185001
[16] Tsai H S, Hsiao C H, Chen C W, Ouyang H and Liang J H 2016 *Nanoscale* **8** 9488
[17] Reinig P, Fenske F, Selle B, Bohne W, Rohrich J, Sieber I and Fuhs W 2004 *Appl. Surf. Sci.* **227** 114
[18] Fenske F, Schulze S, Hietschold M and Schmidbauer M 2008 *Thin Solid Films* **516** 4777
[19] Plantin P, Challali F, Carriot O, Lainata F, Ancilotti M, Gadot G and Brault P 2008 *Microelectron. Eng.* **85** 636
[20] Fujimura S, Someya T, Yoshiba S, Tsukamoto T, Kamisako K and Suda Y 2015 *Jpn. J. Appl. Phys.* **54** 08KD01
[21] Huang F P, Ye C, He H J, Liu Y, Wang X Y and Ning Z Y 2014 *Plasma Sources Sci. Technol.* **23** 015003
[22] He H J, Ye C, Wang X Y, Huang F P and Liu Y 2014 *ECS J. Solid State Sci. Technol.* **3** Q74
[23] Ostrikov K, Neyts E C and Meyyappan M 2013 *Adv. Phys.* **62** 113
[24] Ye C, He H J, Huang F P, Liu Y and Wang X Y 2014 *Phys. Plasma* **21** 043509
[25] Hung F Y, Lui T S, Hu Z S, Chang S J, Chen L H and Chen K J 2012 *Mater. Trans.* **53** 2049
[26] Yang L, Chen Q, Sang L, Wang Z and Liu Z 2013 *Surf. Coat. Technol.* **228** S28
[27] Cinquanta E, Scalise E, Chiappe D, Grazianetti C, Broek B, Houssa M, Fanciulli M and Molle A 2013 *J. Phys. Chem. C* **117** 16719